JOURNAL OF GEOPHYSICAL RESEARCH, VOL. 106, NO. A12, PAGES 28,857–28,865, DECEMBER 1, 2001

Theoretical predictions of the effect of cusp and dayside precipitation on the polar ionosphere

Aurélie Vontrat-Reberac and Dominique Fontaine

Centre d'étude des Environnements Terrestre et Planétaires, Vélizy, France

Pierre-Louis Blelly

Centre d'Etude Spatiale des Rayonnements, Toulouse, France

Marina Galand

Center for Space Physics, Boston University, Boston, Massachusetts, USA

Abstract. We use the numerical model TRANSCAR to investigate the signature of cusp electron and proton precipitation on all ionospheric parameters (electron density, electron and ion temperatures, and ion field-aligned velocity) and to compare it to that of other precipitation source regions expected in the dayside polar ionosphere, such as the low-latitude boundary layer or the dayside extension of the plasma sheet. If the precipitating energetic protons contribute to the formation of a strong density peak in the *E* region, similarly to the auroral zone, the low-energy electrons are responsible for very different features. For example, they produce density enhancements in *F* and low *F* regions which even increase in time owing to a buildup effect induced by the long timescales in this altitude range. We have estimated that cusp electron precipitations heat the ambient electron gas by typically 750–1000 K and induce much larger temperatures than precipitations from any other source regions. One striking feature is the ion upward flows that can reach values up to 250 m s^{-1} or more, well above those obtained from the other source regions. Finally, the electron density enhancement initially produced by cusp precipitation persists for timescales of the order of hours after the precipitation event owing to the long timescales at *F* region altitudes. Combined with transport processes, this effect may supply ionization to other regions of the polar or auroral ionosphere.

1. Introduction

In winter, with at best a very oblique solar illumination, the polar ionosphere sounded by incoherent scatter radars is predicted to be rather depleted. However, observations from the Eiscat Svalbard Radar (ESR) or Søndre Strømfjord reveal numbers of structures with high electron densities which can cover a wide altitude range [*Valladares et al.*, 1989; *Watermann et al.*, 1992; *Nilsson et al.*, 1996; *McCrea et al.*, 2000]. Intense signatures also appear in the temperature and velocity profiles, but their correlation with the density structures is not always obvious. In these cases the ionization production depends on other sources than the reduced solar illumination, mainly, the magnetospheric particle precipitation or, in the *F* region, ionization transport from lower latitudes, better illuminated by the Sun. In this paper we focus on the effects of particle precipitation into the dayside polar ionosphere.

The large number of radar, optical, and magnetic observations at auroral latitudes collected for several decades has motivated the development of theoretical and numerical works on the precipitation process. After the first works by *Rees* [1963] and *Roble and Rees* [1977], various studies concentrated on auroral precipitations. They quantified the energy degradation of the plasma sheet electrons and ions penetrating the high atmospheric layers, the altitude range and the rate of the ionization production, and the heating of the thermal plasma as a function of the incoming particle flux and energy [*Rees*, 1987; *Strickland et al.*, 1993; *Kirkwood and Osepian*, 1995; *Galand et al.*, 1999; *Su et al.*, 1999].

The polar ionosphere has been explored more recently. On the dayside it is connected to the cusp region or to the boundary layers, and the precipitation fluxes from these regions present quite different characteristics from the auroral zone. In the cusp the average electron energy is typically of the order of few hundred eV, as compared to a few keV in the auroral zone. Consequently, the energy deposition occurs in the *F* region and not in the *E* region as for keV electrons [*Stamnes et al.*, 1985]. The protons remain energetic in the cusp, up to a few keV, and their fluxes can even reach larger intensities than in the auroral zone. *Galand et al.* [1999, 2001] showed that intense fluxes of energetic protons produce significant ionization in the *E* region. In the cusp they are expected to be responsible for the whole production below 160-km altitude. From simulations of the cusp precipitation effects on various ionospheric species, *Millward et al.* [1999] similarly concluded that both ion and electron precipitation are important sources of ionization but at markedly different altitudes depending on their energy. One reason is the energy difference between the precipitating electrons and protons, but it is not the only one. Electrons and protons deposit their energy in a different way. The ionization peak is more

Copyright 2001 by the American Geophysical Union.

Paper number 2001JA900131.
0148-0227/01/2001JA900131$09.00

sensitive to altitude for electrons than for ions [*Galand and Richmond*, 2001]. Effects of cusp precipitation should concern other plasma parameters, in particular, the electron temperature, but they have been much less investigated than the ionization production.

In the daytime the polar radars are expected to observe the ionospheric footprints of the cusp and also of the surrounding regions such as the low-latitude boundary layer (LLBL) or the dayside extension of the plasma sheet or its boundary (BPS), depending on solar wind conditions and local time. These regions have been well identified by polar satellites. In particular, the observations by the satellites Defense Meteorological Satellite Program (DMSP) and Polar have provided statistical estimates of the precipitation energy and flux as a function of the geographical location, of the local time, of the season, and of the geomagnetic activity [*Hardy et al.*, 1985, 1989; *Newell and Meng*, 1992; *Liou et al.*, 2001]. Up to now, there is no clear estimate either of their characteristic signatures nor of their differences into the ionosphere.

In this study we proceed similarly to previous theoretical works but with the main objective to simulate the precipitation effects on the dayside polar ionosphere: not only on the electron density profiles but also on the other ionospheric parameters measured by radars, such as the temperatures or field-aligned velocities. We especially emphasize the respective effects due to the precipitating electrons and ions. In this framework we examine the ionospheric signatures of typical precipitations expected in the dayside polar ionosphere from different magnetospheric regions (cusp, LLBL, and BPS), and we compare their signatures. To do this we use the fluid ionospheric model called TRANSCAR, developed and calibrated with European Incoherent SCATter (EISCAT) observations by *Blelly et al.* [1996a, 1996b]. For the various ionospheric species a fluid approach is adopted along magnetic field lines using a 13-moment approximation of Boltzmann's equation. The effects of primary and secondary electrons are taken into account self-consistently through a coupled electron transport model [*Lummerzheim and Lilensten*, 1994]. The proton contribution to electron and ion production is assessed using a proton transport model [*Galand et al.*, 1997] and is input to TRANSCAR. Before presenting and discussing the precipitation signatures (sections 3 and 4), we define a realistic profile of the quiet polar ionosphere (section 2).

2. Quiet Polar Ionosphere

Presently, several empirical models (*Bent et al.* [1972], *Chiu* [1975], *Anderson et al.* [1985, 1989], the International Reference Ionosphere (IRI): *Rawer et al.*, [1978] and *Bilitza et al.*, [1993], for example) provide a description of the middle- and low-latitude ionosphere for magnetically quiet conditions. Empirical models for higher latitudes lack a significant data base, especially for the polar ionosphere, and moreover, a number of phenomena and variable parameters (electric fields, particle precipitations, etc.) have to be taken into account. Presently, these models infer ionospheric profiles at polar latitudes by extension from lower latitudes.

To get a realistic description of the quiet polar ionosphere at polar latitudes, we have used observations by the EISCAT Svalbard Radar (ESR) at the geographic location (78°09'N, 16°03'E) corresponding to an invariant latitude of ~75° [*Wannberg et al.*, 1997]. On February 1, 1998 around 0700 UT, the daily flux of 10.7-cm solar radiation was 86.9, and the geomagnetic daily index *Ap* was ~12. The very weak values observed by ESR for all plasma parameters suggest that the solar illumination, even reduced, is the dominant ionization source (solar zenith angle around 101° at this time). This was confirmed by the low-altitude satellite DMSP-F11, simultaneously in close conjunction with ESR, which measured very weak particle fluxes, less than 0.05 mW m^{-2}. ESR observations, analyzed with GUISDAP [*Lehtinen and Huuskonen*, 1996] and averaged over 3 min during the quiet period, are displayed in Figure 1. The electron density is quite below 10^{11} m^{-3} at the *F* region peak, and the other parameters are also weak and noisy above 400-500 km altitude.

To fit the observations the TRANSCAR model is run for 1 hour, the time interval required to reach steady state [*Roble and Rees*, 1977]. The best fit is obtained by adjusting several parameters [*Blelly et al.*, 1996b], including (1) correction factors to the neutral atmosphere model [*Hedin*, 1991; *Hedin et al.*, 1991] with $C_{[O]}$ (atomic oxygen) = 1.3, $C_{[M]}$ (atomic nitrogen and molecular (O_2 and N_2)) = 1.7, dT_∞ (exospheric temperature deviation) = -70 K, and dU_∞ (exospheric neutral meridional wind deviation) = -400 m s^{-1}; (2) a topside electron heat flow estimated to 8.10^{-4} mW m^{-2} downward; (3) the precipitation fluxes, here simultaneously measured by DMSP-F11; and (4) no electric field, as suggested by the weak ion temperatures.

The simulation results are displayed by the solid line in Figure 1 by comparison to ESR observations. The density profile is fairly well fitted, especially the altitude and shape of the *F* region peak (Figure 1a). The simulation also reproduces very well the electron temperature profile (Figure 1b). For all parameters the data become noisy above 400-500 km, and the fit passes roughly between the data points. The measured profiles for the ion temperature and the ion field-aligned velocity (Figures 1c and 1d) seem more scattered and less well fitted by the numerical results. However, it is not crucial because the values are weak: ~800 K for the ion temperature and 0 ± 50 m s^{-1} for the velocity around the *F* region peak. We have checked afterward that these values did not modify the numerical profiles due to precipitation. These fits reproduce satisfactorily ESR observed profiles of the different ionospheric parameters. In the following we consider them as representative of the quiet state of the dayside polar ionosphere before the occurrence of significant precipitation fluxes.

3. Effects of Electron and Proton Precipitation Into the Dayside Polar Ionosphere

On the dayside the polar ionosphere sounded by ESR can be connected to the cusp or to neighboring regions such as the boundary layers or the dayside extension of the plasma sheet [*Newell et al.*, 1991]. These regions are quite different in terms of particle energies and fluxes. In the following, we have considered typical values for each source region. We are aware that these values depend on the time, the season, the magnetic activity, etc. [*Hardy et al.*, 1985, 1989; *Liou et al.*, 2001]. This theoretical study does not aim to analyze the effects of these factors but rather to give typical orders of magnitude for each source region. The following values have been calculated using the average energy and total particle flux from the statistical precipitation models by *Hardy et al.* [1985, 1989] in the 9-15 MLT time interval, at high latitudes, and for a *Kp* index equal to 3: Cusp (source region 1): Q_{0e} = 0.3 mW m^{-2}, E_{0e} = 70 eV, Q_{0p} = 0.6 mW m^{-2}, E_{0p} = 750 eV; LLBL (source region 2): Q_{0e} = 0.2 mW m^{-2}, E_{0e} = 150 eV, Q_{0p} = 0.3 mW m^{-2},

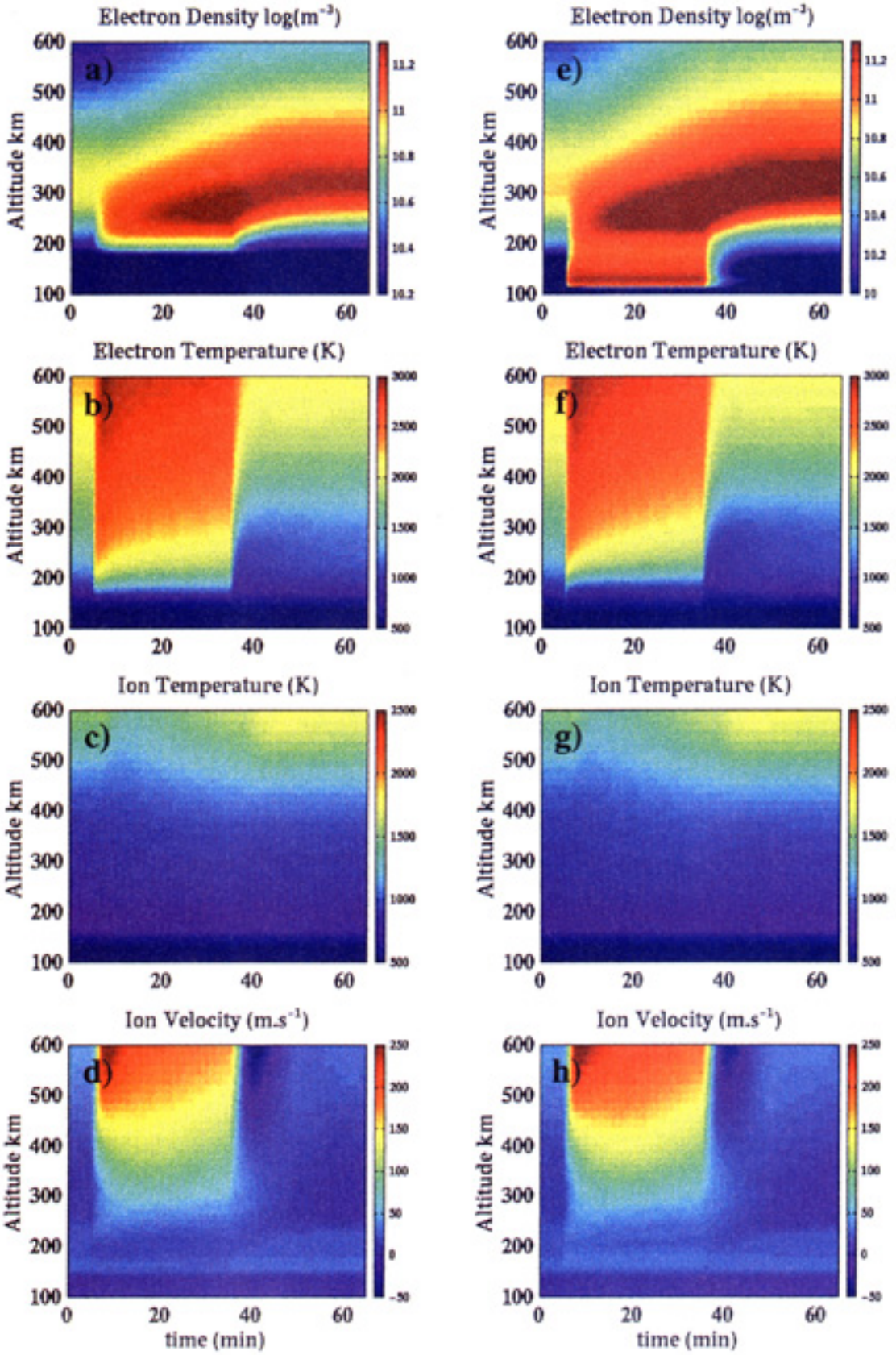

Plate 1. The panels show the altitude-time profiles of (a, b) the electron density, (c-f) electron and ion temperatures, and (g, h) ion field-aligned velocity in response to precipitations for 30 min of only cusp electrons (left column) and of both electrons and protons (right column).

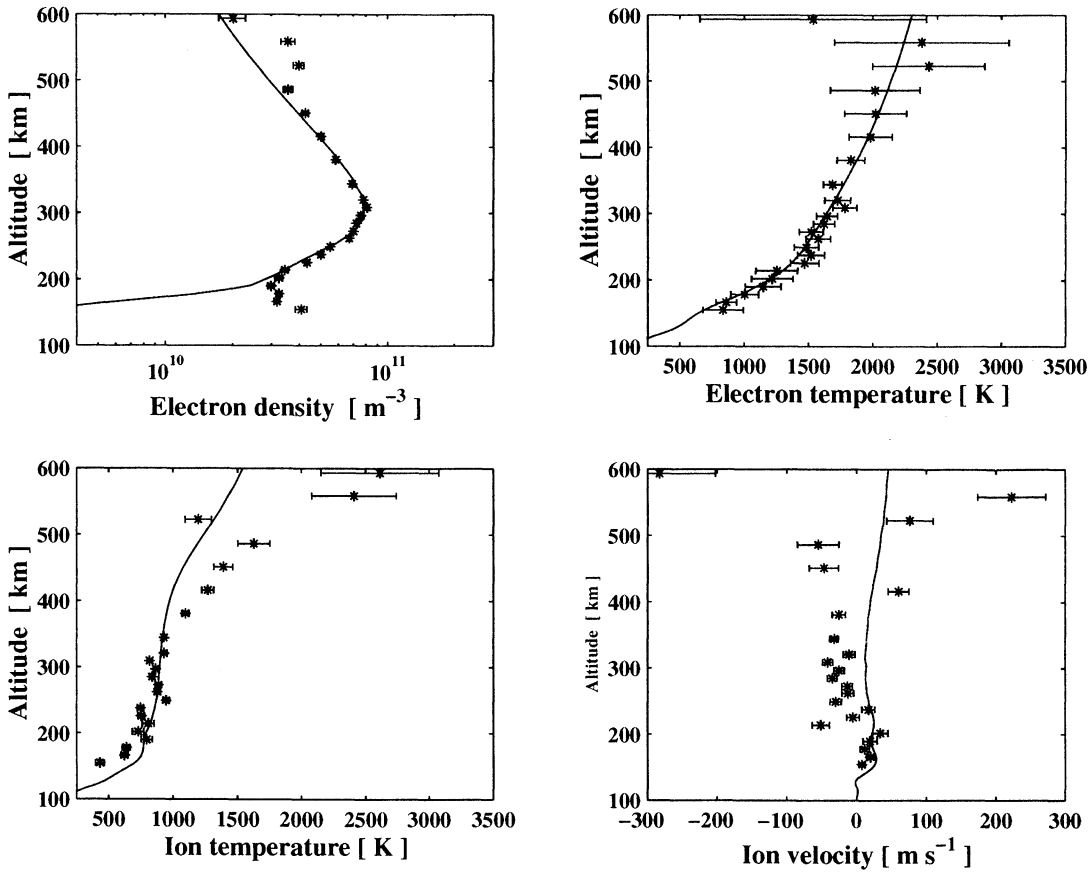

Figure 1. Comparison between Eiscat Svalbard Radar (ESR) observations (stars with error bars) and the modeling results (solid lines) for February 1, 1998, around 0700 UT (quiet ionosphere). Height profiles between 100 and 600 km for (a) electron density, (b) electron temperature, (c) O^+ ion temperature and (d) O^+ ion field-aligned velocity.

E_{0p} = 1.5 keV; BPS (source region 3): Q_{0e} = 0.5 mW m^{-2}, E_{0e} = 400 eV, Q_{0p} = 0.2 mW m^{-2}, E_{0p} = 5.6 keV.

The characteristic energy flux for electrons (Q_{0e}) and for protons (Q_{0p}) is obtained by integration of the total energy flux over all pitch angles. It should be noted that like previous numerical works, we use here the characteristic energy for electrons (E_{0e}) and protons (E_{0p}). Fitting data with a Maxwellian distribution, E_0 is half of the mean energy.

The characteristic energies vary from weak values in the cusp to higher values in the BPS. In terms of energy fluxes the dominant feature is the intense values of proton fluxes in the cusp.

As already well known from the auroral zone, the precipitation fluxes contribute to produce ionization and to heat the ambient ionospheric plasma. Starting from the quiet ionosphere observed on February 1, 1998, and modeled in section 2, we switch on a precipitation source for 30 min at the top of the ionosphere, and we examine the resulting variations of the ionospheric parameters. All other atmospheric parameters remain unchanged. The electric field is taken equal to zero in order to avoid mixing the local signature of precipitations with electric field effects, which will be discussed in section 4. We first focus on the quantitative evaluation of the cusp electron and proton precipitation signatures on the ionospheric parameters observed by EISCAT-ESR, before addressing the cases of the other precipitation sources.

3.1. Cusp Precipitation Case

During the first 5 min we simulate the polar ionosphere at the quiet state modeled in section 1 and then we switch on, at the top of the ionosphere and for 30 min, a constant source of cusp precipitations (source region 1). At t = 35 min the precipitations stop, and the ionosphere evolves on its own.

Plate 1 displays the time dynamics of the altitude profiles of the ionospheric parameters (electron density, electron and ion temperatures, and ion drift velocity) in response to only electron precipitation (left column) and to combined electron and proton precipitation (right column).

At much weaker energies than in the auroral zone, cusp electron fluxes do not reach the E region and produce ionization mainly between 200- and 300-km altitude [*Millward et al.*, 1999], as illustrated in Plate 1a. At these altitudes the characteristic timescales have increased to more than 30 min, as compared to a few seconds for the recombination time in E region. Therefore the continuous precipitation is responsible for a nonsteady density buildup in the F region. After 30 min the layer becomes 300 km thick from 200-km altitude, and the density increases by a factor 3.5, reaching 2.5 10^{11} m^{-3}, before starting to slowly decrease from the low altitudes once the precipitation process stops. Plate 1b shows that the combined effect of both electron and proton precipitations does not significantly modify the F region structure. The density has

gained a factor 3.75, hardly exceeding the factor due to the electrons alone. The cusp proton precipitation is an important source of ionization below 200-km altitude [*Lilensten and Galand*, 1998; *Millward et al.*, 1999]. As illustrated in Plate 1b, it immediately creates an *E* region with a density peak of ~2.10^{11} m^{-3} at about 125-km altitude, the altitude of maximum ionization production for protons of a few keV [*Galand et al.*, 1999]. Finally, the transition region between *E* and *F* region peaks appears as a well-ionized region with significant densities around 10^{11} m^{-3}.

The friction with secondary electrons produced by the precipitation process contributes to heat the ambient thermal electrons. Plate 1c shows that the electron precipitation alone is responsible for an electron temperature enhancement of the order of 1000 K above 220-km altitude, which is the altitude of the maximum energy deposition for cusp electrons. This instantaneous effect permanently accompanies the precipitation process and should produce a constant heating during the precipitation period. However, after the initial increase the electron heating slightly reduces with time as the *F* region density increases. The reason for such a decrease is that the energy quantity supplied by precipitation is shared between an increasing number of ionospheric electrons, which leads to a decrease of the heating. Since the protons mainly produce electrons in the *E* region, they do not account for *F* region electron heating. However, a brief electron heating of 750 K appears around 150 km, the altitude of the maximum of proton energy deposition. However, as illustrated in Plate 1d, it only subsists for a few seconds before the rapid formation of the dense *E* and low *F* regions which cancels it out.

As illustrated in Plate 1e and 1f, the precipitation process has no effect on the ion temperature in the *F* region. In the absence of electric field the ions are predominantly thermalized by the neutrals. This is not the case for the field-aligned velocity of the O^+ ions. Plate 1g and 1h display intense upflows of more than 250 m s^{-1} at the highest altitudes during the precipitation period. The low energy of the precipitating cusp electrons induces an ionization production in the *F* region, i.e., at higher altitude than in auroral zone and a stronger heating of *F* region electrons. Stronger pressure gradients are responsible for an upward acceleration of the ambient O^+ ions to much larger values than expected in auroral zone. The intense electron heating at the beginning of the precipitation period plays probably a dominant role in triggering these intense upward flows, while the density gradients could dominantly do it for the rest of the period. As illustrated in Plate 1h, the small additional effect due to proton precipitation leads to a slightly larger acceleration without modifying the upflows structure.

In summary, the energy difference between electrons and protons precipitating from the cusp leads to an altitude separation of their proper characteristic signature. Below 200 km the intense fluxes of energetic protons play a determinant role in (1) the formation of a dense *E* and low *F* region, (2) a brief electron heating of 750 K, which persists for a few seconds at the beginning of the precipitation period, and (3) the rapid disappearance of any electron heating.

Above 200 km, the low-energy electrons mainly account for (1) an electron density buildup between 200- and 300-km altitude, which can gain a factor 4 for 30 min of continuous precipitation, (2) the progressive formation with time of a much thicker *F* region layer, which typically extends from 200 to 500 km and persists after the precipitation event for time scale of the order of the hour, (3) a very strong electron heating of 1000 K with temperatures exceeding 3000 K in *F* region, and (4) intense O^+ upflows of more than 250 m s^{-1} in *F* region.

3.2. Signatures of Particle Precipitations From LLBL and Plasma Sheet

We now examine the signature of precipitations from other source regions, the LLBL and the dayside extension of the plasma sheet, generally located close to the cusp. Similarly to the cusp case, we simulate the quiet ionosphere, as described in section 2, and then we assume that it is submitted in the same conditions to the source region 2 (LLBL) and 3 (BPS).

Figure 2 displays the height profile of the electron density after 2 min of particle precipitation from LLBL and BPS by comparison to the quiet ionosphere and to the case of cusp precipitation in the same conditions.

In all cases the precipitating energetic protons contribute to enhance the electron density below 150-km altitude and to create an *E* region peak. All *E* region density peaks are similar: Their altitude only varies within a small altitude range, between 115- and 130-km altitude, due to the close values of the characteristic energy of the incident protons. The peak value depends on the incident fluxes. Larger fluxes in the cusp are expected to produce a more intense peak.

In the transition region between the *E* and *F* region peaks, Figure 2 clearly shows the increasing altitude of the production maximum, around 180 km, 200 km, and 230 km, respectively. They correspond to electron precipitations with decreasing energies from source regions 3 (BPS), 2 (LLBL) to 1 (cusp). In the case of precipitation from source regions 2 or 3, the density maximum is somewhat weaker than the cusp maximum which already exceeds 10^{11} m^{-3}. This difference becomes even larger with time: The increase with altitude of the characteristic timescale from seconds in *E* region to typically 1 hour in *F* region gives more time to the ionization for building up. Almost negligible for BPS precipitation, the buildup effect additionally enhances the electron density above the values

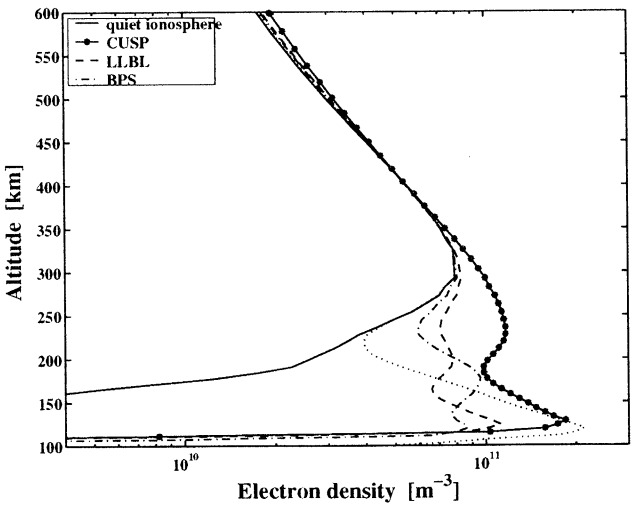

Figure 2. Electron density height profile between 100 and 600 km in an initially quiet ionosphere (thin solid line) and after 2 min of particle precipitations from cusps (dotted solid line), low-latitude boundary layer (LLBL) (dashed line), and dayside extension of the boundary plasma sheet (BPS) (dash-dotted line). By comparison, the thin dotted line shows a profile due to auroral precipitation.

due to the instantaneous production by a factor of 2 after 30 min of precipitation for LLBL and of 4 as already mentioned for the cusp.

Cusp precipitation also contributes to increase the thickness of the F region layer which expands toward higher altitudes (see Plate 1). This effect, which becomes noticeable after a few minutes of continuous precipitation, does not clearly appear in the case of LLBL precipitation or for BPS precipitation.

By comparison, the thin dotted line in Figure 2 represents the electron density profile obtained in response to typical auroral precipitations with large fluxes (Q_{0e}=Q_{0p} = 1 mW m^{-2}) of energetic particles (E_{0e} = 2 keV, E_{0p} = 5.6 keV). They do not affect the F region. In E region they produce a peak comparable to the effect of energetic protons from the previous source regions. It is well separated from the F region peak by a deep minimum between 200- and 250-km altitude, while in the same altitude range, cusp precipitations are precisely responsible for the formation of a maximum. Even in the case of sources 2 and 3, the transition region between the E and F region peaks appears as a well-ionized region, about twice denser than in auroral zone. Another difference is the immediate effect of auroral precipitations on the density profile. They immediately recover the quiet values when the precipitation event stops, because they contribute to ionization only below 200 km. Cusp precipitations, and to a less extent LLBL precipitations, additionally produce ionization in F region which persists for tens of minutes to hours after the precipitation event.

As for cusp precipitation, particle precipitation from the other source regions also contributes to heat the ambient electron gas and to trigger ion upflows. Unlike the signatures on the F region density, the responses on electron temperature and ion velocity are instantaneous, depending on the presence (or not) of precipitation. In a format similar to Figure 2, Figure 3 displays the height profile of the electron temperature after 2 min of continuous precipitation from the different source regions by comparison to the initially quiet ionosphere (thin solid line). BPS and LLBL precipitations contribute to heat the ambient electrons by ~250 K and 300 K, respectively. The electron temperature profiles hardly reach 2500 K in F region. With a heating of 1000 K, cusp precipitations induce electron temperatures of the order of 3000 K and more. This shows that the electron heating increases when the precipitation energy decreases. The electron temperature also depends on the

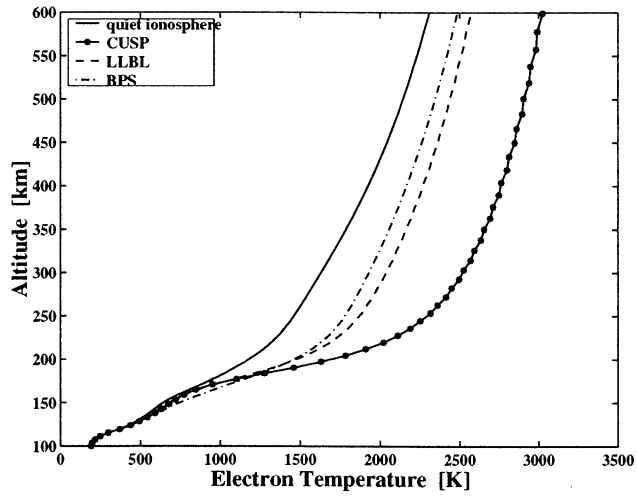

Figure 3. Similar to Figure 2 but for the electron temperature.

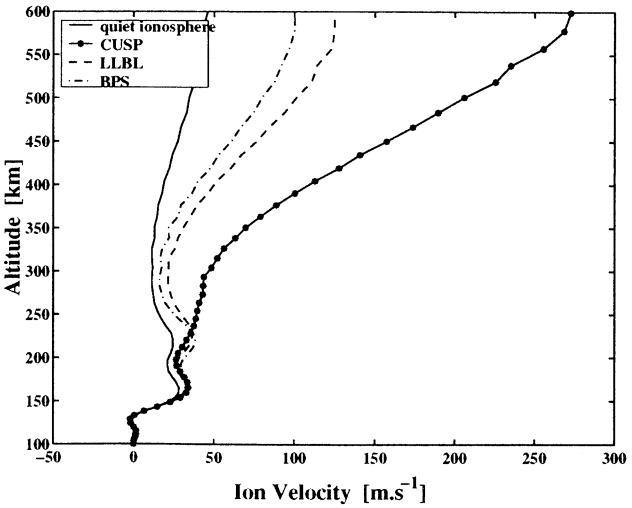

Figure 4. Similar to Figure 2 but for the ion field-aligned velocity.

incident energy flux of the precipitating particles. Finally, we have found that the ratio Q_0 (mW m^{-2})/E_0 (keV) is a good proxy for comparing the amount of electron heating induced by the different precipitations, all other parameters remaining unchanged. This is in agreement with *Su et al.* [1999], who showed that an increase of the number of precipitating electrons as the characteristic energy decreases clearly enhances the electron temperature. The precipitation signatures on the O^+ field-aligned velocity are illustrated in Figure 4. Two minutes of continuous precipitation from BPS and LLBL induce ion upflows of the order of 100 m s^{-1} and 120 m s^{-1}, respectively, at about 500-km altitude. These values largely exceed the weak values, typically below 40 m s^{-1}, observed for the quiet ionosphere (thin solid line). Note that cusp precipitation has a remarkable effect ion upflows, triggering them up to values larger than 250 m s^{-1}. As already mentioned, this effect can be attributed to the low energy of precipitating electrons: Their ionization production and heating in F region are favorable factors to produce strong pressure gradients which accelerate the ionospheric ions O^+ upward due to an enhanced ambipolar electric field [*Su et al.*, 1999].

In summary, the protons from the different precipitation source regions (Cusp, LLBL, and BPS) are responsible for the formation of the E region peak, similarly to the energetic particles precipitating in the auroral zone. The most noticeable difference between the three regions is a larger peak density for cusp protons due to larger incident fluxes. Unlike for the auroral zone, the transition region between the E and F regions, located typically between 150 and 250 km, appears as a dense region. The differences between the different precipitation source regions in this altitude range come from the precipitating electron energy: Lower-energy electrons produce ionization at higher altitudes where the long timescale results in an even larger density enhancement by a buildup effect during the precipitation period. In the same way, when precipitation is turned off, the ionization persists over time periods increasing with altitude, from tens of minutes around 250-km altitude to hours at higher altitudes. It lasts for shorter periods after LLBL precipitation and becomes negligible after BPS precipitation due to the fast recombination at lower altitudes. All sources contribute to heat the ambient electrons and to trigger ion upflows. These effects are much more intense in the case of cusp precipitation.

4. Discussions and Conclusions

With typical values for precipitation from the different magnetospheric regions connected to the dayside polar ionosphere, we have shown that the signature of cusp precipitation dominates all others by the magnitude of the ionospheric parameters that it induces. However, it is conceivable that the fluxes from the other source regions might occasionally intensify above the usual values considered here and also produce intense signatures. We have tested this assumption by simulating large fluxes from the BPS. The ambient electron gas was heated above the values given in section 3, closely approaching temperatures expected for cusp precipitation. The O^+ upward flows were also enhanced, but they did not reach the level of the cusp case. The main differences concerned the density profile: It presented a very dense low *F* region down to 150-km altitude and no ionization production at higher altitude, thus avoiding the confusion with the signature of cusp precipitation.

Note that both electron heating and ion upflows given in section 3 represent a lower limit only. The reason is that particle precipitation into the ionosphere cannot only be considered as the simple supply of energetic particles to the ionospheric plasma. It also involves an energy transfer from the magnetosphere into the ionosphere. Thermal conduction is particularly important above the *F* region peak and governs the electron temperature structure in this altitude range. From EISCAT observations at high altitude, *Blelly and Alcayde* [1994] inferred that the topside heat flux could gain one order of magnitude or more in presence of particle precipitation. In our simulations the topside heat flux is maintained at the level fitted for the quiet ionosphere. Realistic values for the heat flow would contribute to still increase both electron heating and ion upflows in *F* region. We have tested this assumption by simulating a topside heat flux multiplied by 8 during a period of cusp precipitation. The electron temperature profile remained unchanged below 300-km altitude, but a stronger heating occurred above: At 500-km altitude the electron temperature exceeded 4000 K. The O^+ field-aligned velocity, related to the electron pressure gradient, behaved similarly and reached 450 m s^{-1} at 500-km altitude. These large values represent another factor which increases the difference of cusp precipitation with the other source regions.

In this study we did not consider the presence of perpendicular electric fields, which have important effects in the *F* region. One of them is the local heating of the ambient ion gas by increased friction with the neutral gas [*Rees and Walker*, 1968]. It has also been demonstrated that the presence of large perpendicular electric fields, and thus of increased ion temperatures, locally accelerates the chemical reactions depleting the O^+ density and producing NO^+ ions [*Megill and Carleton*, 1964; *Schunk et al.*, 1975]. As a result, the electron density decreases in *F*2 region and induces, in turn, an enhancement of the electron temperature [*Kagan et al.*, 1996]. We reproduced these features by including a perpendicular electric field of 60 mV m^{-1} in our simulations: The ion temperature was enhanced by typically 1200 K, the O^+ density at the *F* region peak reduced by a factor of 2, creating an electron density trough and thus resulting in an enhancement by almost 500 K of the electron temperature above the *F* region peak. Although it was not a direct effect, an upward acceleration of the O^+ ions was also observed for a few minutes associated with electron density gradients [*Blelly et al.*, 1996c]. Finally, electric fields have also nonlocal effects, such as the ionization transport from or to other regions: this effect strongly contributes to the structure of the *F* region density. In summary, the presence of perpendicular electric fields during precipitation events does not fundamentally modify the structure of the *E* region or of the transition region between the *E* and *F* region peaks, unlike the *F* region where it causes dramatic effects: (1) an instantaneous increase of ion temperatures, (2) unpredictable *F* region density profiles because of the competition between an eventually local production by precipitation, the depletion due to accelerated chemical reactions, and the ionization transport from or to other ionospheric regions, and (3) a contribution to the enhancement of electron temperatures and of ion field-aligned velocities for brief periods.

In conclusion, the purpose of this study was primarily to quantitatively estimate the signature of cusp precipitation on the ionospheric parameters observed by radars. We have also investigated its differences with other precipitation source regions expected in the dayside polar ionosphere, i.e., the low-latitude boundary layer (LLBL) and the dayside extension of the plasma sheet (BPS). In order to do this we have used the ionospheric model, called TRANSCAR, developed by *Blelly et al.* [1996a]. As a first step we have achieved a realistic model of the dayside polar ionosphere by fitting ESR observations during a quiet period with TRANSCAR. Then we have switched on sources of electron and also proton precipitation at the topside of the ionosphere, and we have successively examined the cases of precipitation from the different regions.

In agreement with previous predictions by *Galand et al.* [2001], the precipitation of cusp energetic protons has a significant impact on the *E* region electron density with the formation of a peak at some 10^{11} m^{-3}, comparable to the auroral zone. Energetic ions precipitating from LLBL and BPS are also responsible for a similar *E* region peak but probably less intense due to their usually weaker fluxes.

The low-energy electrons precipitating from the cusps produce ionization in the low *F* region typically between 200 and 300 km, as already mentioned by *Millward et al.* [1999]. At these altitudes the characteristic timescale is of the order of 1 hour, the density builds up in time during the precipitation event and rapidly reaches values of the order of several 10^{11} m^{-3}, almost a factor of 4 relative to the quiet values. The differences with the other precipitation source regions come from the larger energies of their precipitating electrons which produce ionization at lower altitudes, around 200 km for LLBL and 180 km for BPS, but still in the transition between *E* and *F* regions. Because of the efficiency of the recombination at lower altitudes, the buildup effect reduces with decreasing altitudes, and the density takes smaller values than in the case of cusp precipitation. In all cases these values exceed the auroral density, depleted in this altitude range. Low-energy electrons precipitating from the cusp have also an expansion effect of the F region toward higher altitudes, resulting in a much thicker *F* layer than that for the quiet ionosphere or for other precipitation source regions. As all processes governing the *F* region density, the additional presence of electric fields would contribute to blur this effect because they transport the *F* region ionization and modify the ionospheric composition.

Except an electron heating which persists a few seconds below 200-km altitude at the beginning of the precipitation period, the energetic protons precipitating from the cusps do not significantly contribute to modify the ionospheric temperatures and velocities. This is not the case for the cusp low-energy electrons. They have a considerable and instantaneous effect on electron heating and on ion acceleration in the *F* region. With a heating of 750–1000 K,

the electron temperature exceeds 3000 K in the *F* region, against ~2500 K for the other source regions. A remarkable effect is that precipitating cusp electrons can trigger intense ion upflows of the order of 250 m s^{-1}, well above the quiet values, usually less than 40 m s^{-1}, and more than twice the upward velocities estimated for BPS and LLBL (~ 120 m s^{-1}). We note that these values should be considered as low limits because the energy flux at the topside of the ionosphere is kept at the level fitted for the quiet ionosphere, while it is known to increase during low-energy precipitation events [*Schunk et al.*, 1986]. Simulations with realistic topside energy flux lead to electron temperatures exceeding 4000 K and ion upflows of 450 m s^{-1} at 500-km altitude. Larger precipitation fluxes from the other source regions may occasionally produce higher electron temperatures and more intense ion upflows than usual. Although it is difficult to reproduce upflows as intense as those for cusp precipitation, the density profile in the transition region between the *E* and *F* region peak gives complementary indications to distinguish between the signatures of the various source regions.

Finally, cusp precipitation into the ionosphere has also long-term consequences. During the precipitation event, low-energy electrons contribute to increase the *F* region density, which builds up with time to reach several 10^{11} m^{-3}, and to expand the *F* layer toward higher altitudes. We have already mentioned that the presence of electric fields would blur this local production, transport it, or at least mix it with other processes. If electric fields do not continuously exist during the event, intense density structures, extended toward higher altitudes, are created by cusp precipitation. These structures persist over time periods of the order of hours after the precipitation event due to long characteristic timescales in the *F* region. Consequently, cusp precipitation should be considered as an ionization source for the polar dayside ionosphere, a rather depleted region because of its weak solar illumination, especially in winter. Moreover, the antisunward flow may transport the ionization across the polar cap and thereby supply the nightside polar and auroral regions.

Acknowledgments. The authors are grateful to the director and staff of the EISCAT Scientific Association for providing the radar facilities and assistance with making the observations. EISCAT is an international association, supported by the research councils of Finland (SA), France (CNRS), the Federal Republic of Germany (MPG), Japan (NIPR), Norway (RCN), Sweden (NFR), and the United Kingdom (PPARC).
Michel Blanc thanks Patrick Newell and Alan Aylward for their assistance in evaluating this paper.

References

Anderson, D. N., M. Mendillo, and B. Herniter, A semi-empirical low-latitude ionospheric model, *Rep. AFGL-TR-85-0254*, Air Force Geophys. Lab., Hanscom Air Force Base, Mass., 1985.

Anderson, D. N., J. M. Forbes, and M. Codrescu, A fully analytical, low- and middle-latitude ionospheric Model, *J. Geophys. Res.*, *94*, 1520, 1989.

Bent, R. B., S. K. Llewellyn, and P. E. Schmid, A highly successful empirical model for the worldwide ionospheric electron density profile, report, DBA Syst., Melbourne, Fla., 1972.

Bilitza, D., K. Rawer, L. Bossy, and T. Gulyaeva, International Reference Ionosphere: Past, Present, Future, *Adv. Space Res. 13*, #3, 3, 1993.

Blelly, P. L., and D. Alcayde, Electron heat flow in the auroral ionosphere inferred from EISCAT-VHF observations, *J. Geophys. Res.*, *99*, 13,181, 1994.

Blelly, P. L., A. Robineau, J. Lilensten, and D. Lummerzheim, 8-moment fluid models of the terrestrial high latitude ionosphere between 100 and 3000 km, in *Solar Terrestrial Energy Program (STEP): Handbook of Ionospheric Models*, edited by R.W. Schunk, pp. 53-72, Utah State University and SCOSTEP-STEP WG-3, 1996a.

Blelly, P.L., J. Lilensten, A. Robineau, J. Fontanari, and D. Alcayde, Calibration of a numerical ionospheric model with EISCAT observations, *Ann. Geophys.*, *14*, 1375, 1996b.

Blelly, P.L., A. Robineau, and D. Alcaydé, Numerical modeling of intermittent ion outflow events above EISCAT, *J. Atmos. Terr. Phys.*, *58*, 273, 1996c.

Chiu, Y. T., An improved phenomenological model of ionospheric density, *J. Atmos. Terr. Phys.*, *37*, 1563, 1975.

Galand, M., and A.D. Richmond, Ionospheric electrical conductances produced by auroral proton precipitation, *J. Geophys. Res.*, *106*, 117, 2001.

Galand, M., J. Lilensten, W. Kofman, and R.B. Sidje, Proton transport model in the ionosphere. Multistream approach of the transport equations, *J. Geophys. Res.*, *102*, 22,261, 1997.

Galand, M., R. G. Roble, and D.Lummerzheim, Ionization by energetic protons in Thermosphere-Ionosphere Electrodynamics General Circulation Model, *J. Geophys. Res.*, *104*, 27,973, 1999.

Galand, M., T.J. Fuller-Rowell, and M.V. Codrescu, Response of the upper atmosphere to auroral protons, *J. Geophys. Res.*, *106*, 127, 2001.

Hardy, D. A., M. S. Gussenhoven, and E. Holeman, A statistical model of the auroral electron precipitation, *J. Geophys. Res.*, *90*, 4229, 1985.

Hardy, D. A., M. S. Gussenhoven, and D. Brautigam, A statistical model of the auroral ion precipitation, *J. Geophys. Res.*, *94*, 370, 1989.

Hedin, A.E., Extension of the MSIS thermosphere model into the middle and lower atmosphere, *J. Geophys. Res.*, *96*, 1159, 1991.

Hedin, A.E. et al., Revised global model of thermosphere winds using satellite and ground-based observations, *J. Geophys. Res.*, *96*, 7657, 1991.

Kagan, L.M., M.C. Kelley, and A. Doe, Ionospheric electron heating by structured electric field: Theory and experiment, *J. Geophys. Res.*, *101*, 10,893, 1996.

Kirkwood, S., and A. Osepian, Quantitative studies of energetic particle precipitation using incoherent scatter radar, *J. Geomagn. Geoelectr.*, *47*, 783, 1995.

Lehtinen, M. and A. Huuskonen, General incoherent scatter analysis and GUISDAP, *J. Atmos. Terr. Phys.*, *58*, 435, 1996.

Lilensten, J., and M. Galand, Proton-electron precipitation effects on the electron production and density above EISCAT (Tromsø) and ESR, *Ann. Geophys.*, *16*, 1299, 1998.

Liou, K., P. T. Newell, and C. I. Meng, Seasonal effects on auroral particle acceleration and precipitation, *J. Geophys. Res.*, *106*, 5531, 2001.

Lummerzheim, D., and J. Lilensten, Electron transport and energy degradation in the ionosphere: Evaluation of the numerical solution, comparison with laboratory experiments and auroral observations, *Ann. Geophys.*, *12*, 1039, 1994.

McCrea, I.W., M. Lockwood, J. Moen, F. Pitout, P. Eglitis, and A.D. Aylward, ESR and EISCAT observations of the response of the cusp and cleft to IMF orientation changes, *Ann. Geophys.*, *18*, 1009, 2000.

Megill, L.R., and N.P. Carleton, Excitation by local electric fields in the aurora airglow, *J. Geophys. Res.*, *69*, 101, 1964.

Millward, G. H., R. J. Moffett, H. F. Balmforth, and A.S. Rodger, Modeling the ionospheric effects of ion and electron precipitation in the cusp, *J. Geophys. Res.*, *104*, 24,603, 1999.

Newell, P.T., and C.I. Meng, Mapping the dayside ionosphere to the magnetosphere according to particle precipitation characteristics, *Geophys. Res. Lett.*, *19*, 609, 1992.

Newell, P.T., W.J. Burke, E.R. Sanchez, C.I. Meng, M.E. Greenspan, and C.R. Clauer, The low-latitude boundary layer and the boundary plasma sheet at low altitude: Prenoon precipitation regions and convection reversal boundaries , *J. Geophys. Res.*, *96*, 21,013, 1991.

Nilsson, H., M. Yamauchi, L. Eliasson, and O. Norberg, Ionospheric signature of the cusp as seen by incoherent scatter radar, *J. Geophys. Res.*, *101*, 10947, 1996.

Rawer, K., D. Bilitza, and S. Ramakrishnan, Goals and status of the International Reference Ionosphere, *Rev. Geophys.*, *16*, 177, 1978.

Rees, M.H., Auroral ionization and excitation by incident energetic electrons, *Planet. Space Sci.*, *11*, 1209, 1963.

Rees, M.H., Modeling of the heating and ionizing of the polar thermosphere by magnetospheric electron and ion precipitation, *Phys. Scr.*, *T18*, 249, 1987.

Rees, M.H., and J.C.G. Walker, Ion and electron heating by auroral electric fields, *Ann. Geophys.*, *24*, 193, 1968.

Roble, R.G., and M.H. Rees, Time-dependent studies of the aurora: Effects of particle precipitation on the dynamic morphology of ionospheric and atmospheric properties, *Planet Sci.*, *25*, 991, 1977.

Schunk, R.W., W.J. Raitt, and P.M. Banks, Effect of electric fields on the daytime high-latitude *E* and *F* regions, *J. Geophys. Res.*, *80*, 3121, 1975.

Schunk, R.W., J.J. Sojka, and M.D. Bowline, Theoretical study of the electron temperature in the high-latitude ionosphere for solar maximum and winter conditions, *J. Geophys. Res.*, *91*, 12,041, 1986.

Stamnes, K., M.H. Rees, B.A. Emery, and R.G. Roble, Modeling of cusp auroras: The relative impact of solar EUV radiation and soft electron precipitations, in *The Polar Cusp*, edited by J.A. Holtet and A. Egeland, pp. 137-147, D. Reidel Publishing Company, Dordrecht, Holland, 1985.

Strickland, D.J., R.E. Daniell, J.R. Jasperse, and B. Basu, Transport-theoretic model for the electron-proton-hydrogen atom aurora, *J. Geophys. Res.*, *98*, 21,533, 1993.

Su, Y.-J., R.G. Caton, J.L. Horwitz, and P.G. Richards, Systematic modeling of soft-electron precipitation effects on high-latitude F region and topside ionospheric upflows, *J. Geophys. Res.*, *104*, 153, 1999.

Valladares, C.E., Su. Basu, R.J. Niciejewski, and R.E. Sheehan, Simultaneous radar and satellite observations of the polar cusp/cleft at Sondre Stromfjord, in *Electromagnetic Coupling in the Polar Clefts and Caps*, edited by P. E. Sandholt and A. Egeland, pp. 285-298, Kluwer Acad., Norwell, Mass., 1989.

Wannberg, U.G. et al., The EISCAT Svalbard Radar: A case study in modern incoherent scatter radar system design, *Radio Sci.*, *32*, 2283, 1997.

Watermann, J., O. de la Beaujardière, and P.T. Newell, Incoherent scatter radar observations of ionospheric signatures of cusp-like electron precipitation, *J. Geomagn. Geoelectr.*, *44*, 1195, 1992.

P. L. Blelly, CESR-CNRS/UPS, 9 avenue du Colonel Roche, 31028 Toulouse cedex, France.

D. Fontaine and A. Vontrat-Reberac, CETP-CNRS/UVSQ, 10-12 avenue de l'Europe, 78140 Vélizy, France.

M. Galand, Center for Space Physics, Boston University, Boston, MA 02215, USA. (Pierre-Louis.Blelly@cesr.fr; Dominique.Fontaine @cetp.ipsl.fr; Aurelie.Vontrat@cetp.ipsl.fr; mgaland@pocc.bu.edu)

(Received April 25, 2001; revised August 16, 2001;
accepted August 17, 2001.)